Cleaner Materials 5 (2022) 100099

Contents lists available at ScienceDirect

Cleaner Materials

journal homepage: www.journals.elsevier.com/cleaner-materials

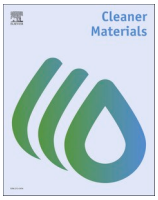

Low-carbon cements: Potential for low-grade calcined clays to form supplementary cementitious materials

Bamdad Ayati [a,*], Darryl Newport [b], Hong Wong [c], Christopher Cheeseman [c]

[a] Sustainability Research Institute, University of East London, London E16 2RD, United Kingdom
[b] Suffolk Sustainability Institute, University of Suffolk, Ipswich IP4 1QJ, United Kingdom
[c] UKRIC Advanced Infrastructure Materials Laboratory, Department of Civil and Environmental Engineering, Imperial College London, SW7 2BU, United Kingdom

ARTICLE INFO

Keywords:
Calcined clays
Pozzolans
Low-carbon cement
Supplementary cementitious materials

ABSTRACT

The use of low-carbon supplementary cementitious materials (SCM), such as calcined clays, to replace cement clinker has been recognized by the Cement Industry to achieve reductions in greenhouse gas emissions. This paper investigates eight low-grade clays, with <20% kaolinite, obtained from different geological formations, that have been calcined to produce potential SCMs. The clays were characterised before and after calcining at 750, 800, 850 and 900 °C, and the mineralogical changes and amorphous phase contents determined. The pozzolanic activity and the strength activity index of the different calcined clays were evaluated. The results show that calcined clays from the Oxford and Ampthill geological formations in the UK can produce SCMs with pozzolanic activity higher than conventional SCMs such as PFA. These clays were rich in illite and smectite and produced ~60% amorphous phase when calcined at 850 °C. Mortars produced using calcined clays had higher compressive strengths than mortars containing pulverised fuel ash and achieved ~90% of the compressive strength of 100% Portland cement mortar samples at 28 days. The research demonstrates that low-grade clay resources can be calcined to produce SCMs and that these can be used to form cementitious materials with reduced total associated CO_2 emissions.

Introduction

Global production of Portland cement (PC) contributes to ~7% of total global anthropogenic CO_2 emissions. The International Energy Agency (IEA) reported that to achieve the 50% target reduction in CO_2 emissions required to limit average global temperature increase to 2 °C, the cement industry needs to reduce direct CO_2 emissions by 24% below current levels (2021) by 2050 (International Energy Agency, 2018). The IEA technological roadmap proposed a number of mitigation strategies that focussed on energy efficiency and alternative fuels in cement kilns, carbon capture and storage and clinker substitution (IEA, 2009). Recent technological improvements to achieve higher energy efficiencies in cement kilns and the use of waste-derived fuels have delivered reductions in CO_2 emissions (Kaddatz et al., 2013; Mirhosseini et al., 2019; Wu et al., 2019). Studies on Carbon Capture and Storage (CCS) from cement kilns have shown promise (Roussanaly et al., 2017; Spinelli et al., 2018), although the technology is expensive ($60/t$CO_2$), particularly given that most future cement production will be in developing countries (Li et al., 2013).

Clinker substitution with supplementary cementitious materials (SCMs) is considered the most viable option for lowering the environmental impact of PC (Environment et al., 2018). The most widely used SCMs have been pulverised fuel ash (PFA) and ground granulated blast furnace slag (GGBFS), the supplies of which are likely to become increasingly problematic in the future. Therefore, there is a need to look for alternative materials that can reduce clinker use and reduce the embodied carbon in concrete.

Calcined clays are receiving much attention as a potential SCM, given that clays are geologically abundant, and calcining is a relatively low-cost, low-carbon, simple process. Clays are often stockpiled in quarries, and they may also be available as overburden, basal deposits or clay excavation wastes. Other sources of clay are becoming available in large quantities as the result of major civil engineering infrastructure projects such as tunnelling and road construction (Zhou et al., 2017; Ayati et al., 2018).

Clays typically contain minerals such as kaolinite, smectite and illite. These may become pozzolanic when calcined at temperature between 700 and 900 °C and this is associated with dehydroxylation reactions

* Corresponding author.
E-mail address: b.ayati@uel.ac.uk (B. Ayati).

https://doi.org/10.1016/j.clema.2022.100099
Received 21 December 2021; Received in revised form 3 March 2022; Accepted 28 May 2022
Available online 31 May 2022

Table 1
List of clay sources and their geological formation: mineralogical composition and amorphous content of clays (as received), PFA and PC (CEM I) used in this study were measured by XRD Rietveld refinement with an internal standard (I: illite, S: smectite, I/S: interstratified illite/smectite, K: kaolinite, Ch: chlorite, Q: quartz, C: calcite, H: Hematite, M: Mullite P: pyrite, G: gypsum).

Sample	Geological Formation	Mineralogy												
		I	S	I/S	K	Ch	Q	C	H	M	P	G	TiO_2	Amorphous
KIM	Kimmeridge Clay	–	–	45.0	5.8	7.0	22.4	5.8	–	–	1.3	–	–	12.7
KEL	Kellaways Clay	–	–	36.5	15.8	0.6	24.9	7.0	–	–	1.0	–	–	13.9
OXF	Oxford Clay	–	–	45.1	12.5	2.7	20.3	5.1	–	–	1.6	–	–	12.8
AMP	Ampthill Clay	–	–	31.3	18.4	5.5	20.0	11.4	0.7	–	1.5	–	–	11.0
GLT	Gault Clay	11.7	30.5	–	8.9	–	20.3	7.1	–	–	3.0	–	–	18.4
LOX	Lower Oxford Clay	5.7	22.2	–	6.0	–	40.1	–	–	–	–	1.2	3.3[R]	21.5
CMS	Coal Measure Shale	28.4[Ph]	–	–	19.0	4.5	43.6	–	3.3	–	–	–	1.1[An]	0.1
ALL	Alluvial Clay	19.9[Ph]	–	–	3.7	11.8	32.8	–	–	–	–	–	5.2[R]	26.5
PFA							11.5			13.1				75.4
		C_3S	C_2S	C_3A	C_4AF	Anhydrite								
PC		63.0	13.4	8.4	10.7	2.6								

[Ph] Phlogopite was identified as the dominant mica.
[R] Rutile polymorph of TiO_2.
[An] Anatase polymorph of TiO_2.

and the formation of amorphous aluminosilicates that react in the presence of hydrating PC to produce calcium silicate hydrate (C-S-H) (Tironi et al., 2013). The majority of research on calcined clays has focused on calcined kaolinitic clays at substitution levels up to 30% and these systems produce similar performance to 100% PC (Sabir et al., 2001; Vizcaíno Andrés et al., 2015; Almenares et al., 2017; Tironi et al., 2017;).

Limestone calcined clay cement (LC3) systems use synergies between calcined clay and limestone and allow up to 50% reductions in clinker use (Krishnan et al., 2019). However, the clays used in LC3 systems normally contain at least 40% kaolinite (Scrivener et al., 2019; Scrivener et al., 2018).

Previous research on calcined low-grade clays in LC3 has shown that longer-term clinker hydration occurs in these systems because availability of portlandite is not a limiting factor (Krishnan et al., 2020). Mica rich clays have been calcined at 900 °C and used to replace 15% by mass of PC without reducing the strength cement (Kaminskas et al., 2018). The suitability of calcining selected German clays for use as SCMs has also been demonstrated (Schulze and Rickert, 2019). The work reported in this paper assesses the potential to produce viable SCMs from low-grade clay deposits with kaolinite contents of <20%. The study focuses on clay samples obtained from major UK clay formations. These have been characterised, calcined, and the mineralogical changes and pozzolanic activity assessed. This is important research because low-grade clays are available in many parts of the world, and these could potentially be used to produce viable SCMs.

Materials and method

The selection of clays for sampling was based on information obtained from quarries across the UK. Eight clays were obtained from the sources given in Table 1. The geological formations of the samples were Kimmeridge Clay (KIM), Kellaways Clay (KEL), Oxford Clay (OXF), Ampthill Clay (AMP), Gault Clay (GLT), Lower-Oxford Clay (LOX), Coal Measure Shale (CMS) and Alluvial Clay (ALL). Each sample was collected from the current working faces of quarries at various locations across the site.

Mineralogical phase identification of the as-received clay samples used X-ray diffraction (XRD). Clay fractions (<2μm) were separated by centrifugation and analysed before and after saturation with ethylene glycol and heat treatment at 400 °C to identify the clay minerals present (Moore and Reynolds, 1989). XRD used a Rigaku Miniflex diffractometer with a θ-θ Bragg-Brentano configuration and Cu-Kα radiation (λ = 1.5418 Å) at 40 kV and 15 mA. Samples were scanned at a rotational speed of 10 rpm in the 2θ range from 3° to 70° at a scanning speed of 2°

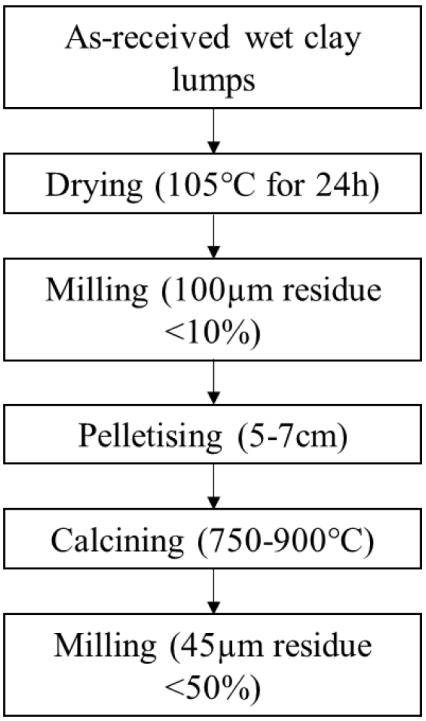

Fig. 1. Process flowchart showing the stages prior to calcination and the follow-up milling regime.

(2θ)/min and step size of 0.02° 2θ. Rietveld quantitative phase analysis was performed using PDXL2 software (version 2.8.3.0). The amorphous content (W_{AM}) was determined by the internal standard method (Madsen et al., 2011) by spiking samples with 50 wt% Al_2O_3 (APC pure, UK) using:

$$W_{AM} = \frac{1 - W_{IS}^{a}/W_{IS}}{100 - W_{IS}^{a}} \times 10^{4} \quad (1)$$

where (W_{IS}^{a}) is the actual weight of the internal standard material in the mix and (W_{IS}) is the weight percent of the internal standard determined from Rietveld refinement (Stetsko et al., 2017).

As-received clay samples were dried at 105 °C for 24 h and milled in a disc mill (Tinius Olsen TO-443) to give a 100 μm residue of <10%. This was formed into pellets (5–7 cm in diameter) by adding water and hand

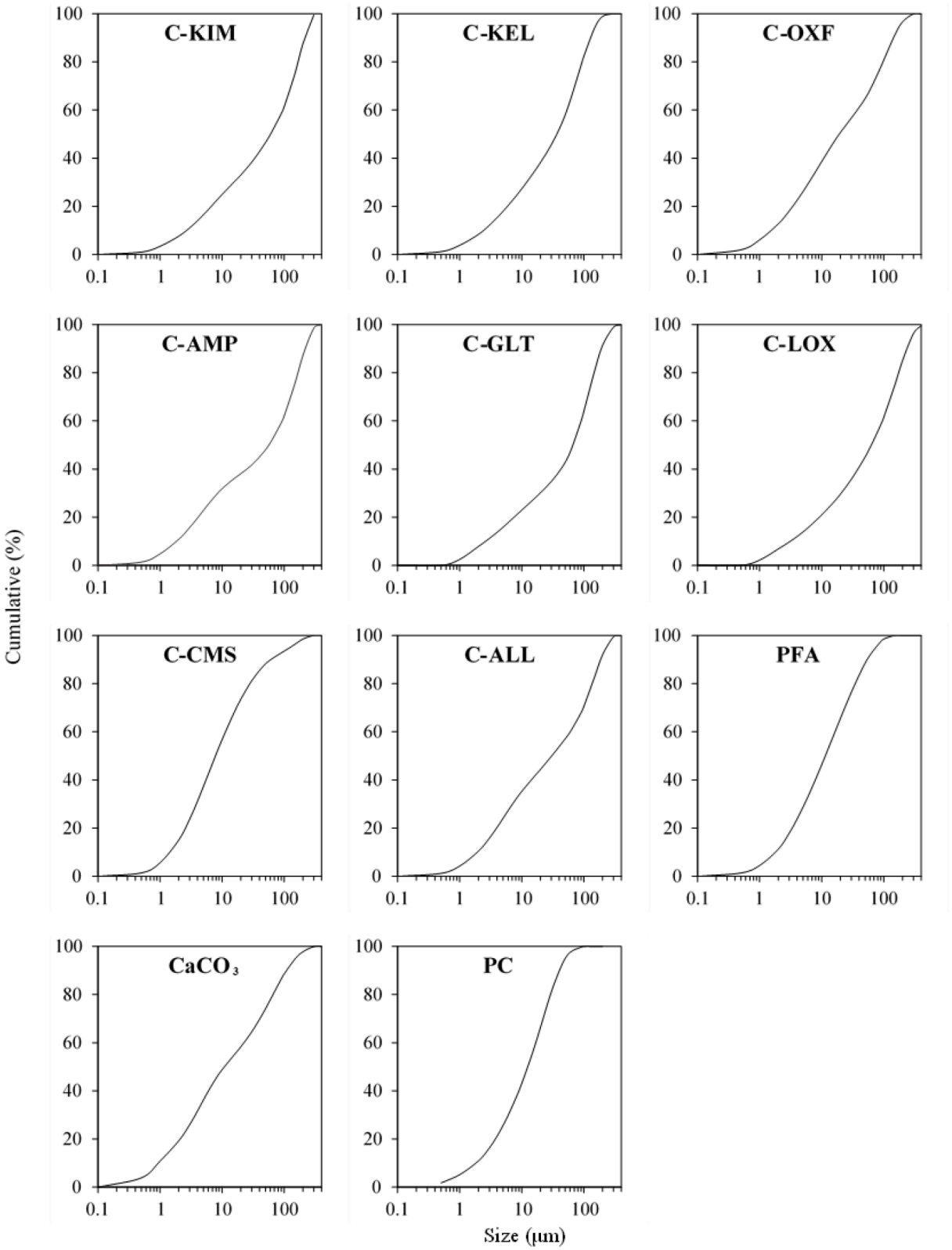

Fig. 2. Particle size distribution of calcined clays (850 °C), PFA, calcium carbonate and PC used in this study. Calcined Kimmeridge Clay, Kellaway Clay, Oxford Clay, Ampthill Clay, Gault Clay, Lower-Oxford Clay, Coal Measure Shale and Alluvial Clay were labelled as (C-KIM), (C-KEL), (C-OXF), (C-AMP), (C-GLT), (C-LOX), (C-CMS) and (C-ALL), respectively.

Table 2
Chemical compositions, fineness and specific surface area (SSA) of calcined clays (850 °C) and PFA.

	C-KIM	C-KEL	C-OXF	C-AMP	C-GLT	C-LOX	C-CMS	C-ALL	PFA
SiO_2	53.84	55.41	54.96	52.74	57.40	65.77	60.96	67.81	58.05
Al_2O_3	19.29	16.61	20.41	19.97	20.64	19.73	21.79	15.91	20.35
Fe_2O_3	6.64	10.13	6.85	6.98	8.36	6.75	8.56	5.35	8.90
Mn_2O_3	0.03	0.06	0.04	0.07	0.05	0.03	0.09	0.08	–
P_2O_5	0.08	0.25	0.13	0.12	0.13	0.06	0.16	0.12	–
TiO_2	0.89	0.92	0.98	0.81	0.83	1.01	1.03	0.77	0.89
CaO	9.76	8.47	6.87	9.83	5.44	1.29	0.51	1.01	2.84
MgO	1.92	1.16	1.50	1.65	2.00	1.35	1.96	3.58	1.73
K_2O	3.63	2.02	3.22	3.52	3.38	2.60	3.63	3.39	1.88
SrO	0.05	0.02	0.03	0.03	0.03	0.01	0.01	0.01	–
SO_3	2.80	3.50	3.06	2.71	0.91	0.37	0.06	0.11	–
Na_2O	0.25	0.29	0.33	0.22	0.21	0.31	0.32	0.63	2.31
LOI	0.64	1.01	1.46	1.52	0.50	0.82	0.99	1.01	1.78
Total + SO_3	99.82	99.85	99.84	100.1	99.88	100.1	100.0	99.78	98.73
Al/Si	0.36	0.30	0.37	0.38	0.36	0.30	0.36	0.23	0.35
45 μm residue (%)	56.5	38.6	28.9	49.3	47.5	48.3	17.8	49.6	8.4
SSA (m^2/g)	0.905	1.020	1.480	1.190	0.725	0.656	1.720	1.190	1.430
d_{50} (μm)	60.4	36.7	19.1	56.4	67.1	63.2	7.8	30.4	11.4

rolling, prior to calcining. Pelletisation produces a reducing environment within the pellets upon heating and cooling, resulting in a matrix phase of mainly Fe^{2+} (grey-black), which produces calcined clays with colour comparable to PC. This is in contrast to calcining loose clay, which produces an oxidising environment constituting mainly Fe^{3+} with a deep red colour that may be undesirable for applications. The process is shown in Fig. 1.

The clays were initially calcined for 60 min at 750, 800, 850 and 900 °C in an electric chamber furnace using a heating rate of 5 °C/min. The optimum calcining temperature was determined using XRD data to evaluate dehydroxylation, the generation of amorphous phases and the recrystallisation of non-reactive phases such as feldspars.

Clay samples calcined at the optimal temperature for maximum reactivity (850 °C) were denoted C-KIM, C-KEL, C-OXF, C-AMP, C-GLT, C-LOX, C-CMS, and C-ALL. These calcined clay samples were ground prior to pozzolanic activity testing. The particle size distribution (PSD) and specific surface area (SSA) of calcined clays, PFA (Cementos Tudela Veguin, SAU), $CaCO_3$ filler (Trucarb 298) and PC (CEM I – Blue Circle – Procem) was determined by laser diffraction (Mastersizer 2000 laser granulometer, Malvern Instruments with Sirocco 2000 dry dispersion unit). Fineness was determined from the > 45 μm residue (Alpine Air Jet Sieves, A 200 LS). The chemical composition of calcined samples was analysed using X-ray fluorescence (XRF) analysis (Malvern Panalytical Axios Max). Calcined clay characterisation data is given in Fig. 2 and Table 2.

The pozzolanic activity test (BS 8615–2:2019) was completed by adding 1 g of calcined clay to 2.0 g of CaO, prepared by heating $CaCO_3$ (Sigma Aldrich) at 1000 °C for 1 h in an Erlenmeyer flask containing 250 ml deionised water maintained at 85 ± 5 °C for 16 h under stirring and flux condition. To prepare the solution for titration, 250 ml of sucrose solution was prepared by dissolving 60 g of sucrose in 250 ml deionised water. This was added to the flask contents, mixed for 15 min, and filtered using Whatman 42 filter paper. 200 ml of the solution was separated for titration against 0.1 N HCl using phenolphthalein as indicator. The amount of $Ca(OH)_2$ in terms of mg fixed per g of pozzolan was calculated using the formula:

$$Ca(OH)_2 = 2 \times \frac{V_1 - V_2}{V_1} \times \frac{74}{56} \times 1000 \quad (2)$$

where V_1 and V_2 are the volume of HCl in ml at the endpoint of titration of the blank and test samples, respectively.

The $Ca(OH)_2$ content of cement pastes containing calcined clays at 7 and 28 days was determined by TGA, from the distinct weight loss that occurs between 450 and 600 °C. The exact temperature range was obtained from derivative weight loss (DTG) data using a tangential method and the weight loss ($WL_{Ca(OH)_2}$) determined by integration of the peak area to calculate the $Ca(OH)_2$ content:

$$Ca(OH)_2 = WL_{Ca(OH)_2} \times \frac{74}{18} \quad (3)$$

Pastes with a water-to-binder (w/b) ratio of 0.50 were prepared using PC with 25% calcined clay substitution. These were sealed in small plastic vials immediately after mixing and stored at 20 °C. After 28 days the vial contents were ground in an agate pestle and mortar under isopropyl alcohol to inhibit further hydration. The samples were then dried in a desiccator at 10% relative humidity and 20 °C. Two control samples, one with PC and the other with 25% $CaCO_3$ filler substitution were prepared to account for dilution and filler effects. TGA (Stanton Redcroft TG1000M) was conducted on 0.02 g of ground sample up to 900 °C.

The strength activity index (SAI) values were determined by measuring the compressive strength of 50 mm mortar cubes after 28 days hydration. Mortar cubes were made with PC and 25% calcined clay substitution and standard sand (1:3) at a w/b ratio of 0.50 following the procedure described in BS EN 196-1 (2005). Cubes with 25% PFA were prepared and tested to compare the performance of calcined clays with a conventional SCM. The SAI values were calculated using:

$$SAI = \frac{A}{B} \times 100\% \quad (4)$$

where A is the average compressive strength (MPa) of test samples and B is the average compressive strength of the control PC sample.

Results

XRD analysis of raw and calcined clays

XRD data of the clay fractions before and after saturation with ethylene glycol and heat treatment at 400 °C are shown in Fig. 3. Most samples show peaks around 6.23°2θ associated to chlorite. This was distinguished from smectites where no expansion to lower angles in ethylene glycol saturated samples occurs, and from vermiculite, where no collapse of the (001) reflection during heat treatments was observed (Poppe et al., 2001).

Illite, smectite and illite/smectite (I/S) mixed-layer minerals were distinguished following changes in the peak shape in ethylene glycol saturated samples (Brime, 2011). The results of XRD/Rietveld phase quantification for as-received clay samples, PFA and PC are shown in Table 1. I/S mixed layers were the dominant clay mineral (30–45%) in clays from Kimmeridge, Kellaways, Oxford and Ampthill formations. Kaolinite and chlorite were present at concentrations below 20% in most samples. Quartz, calcite, hematite, pyrite, gypsum and rutile were

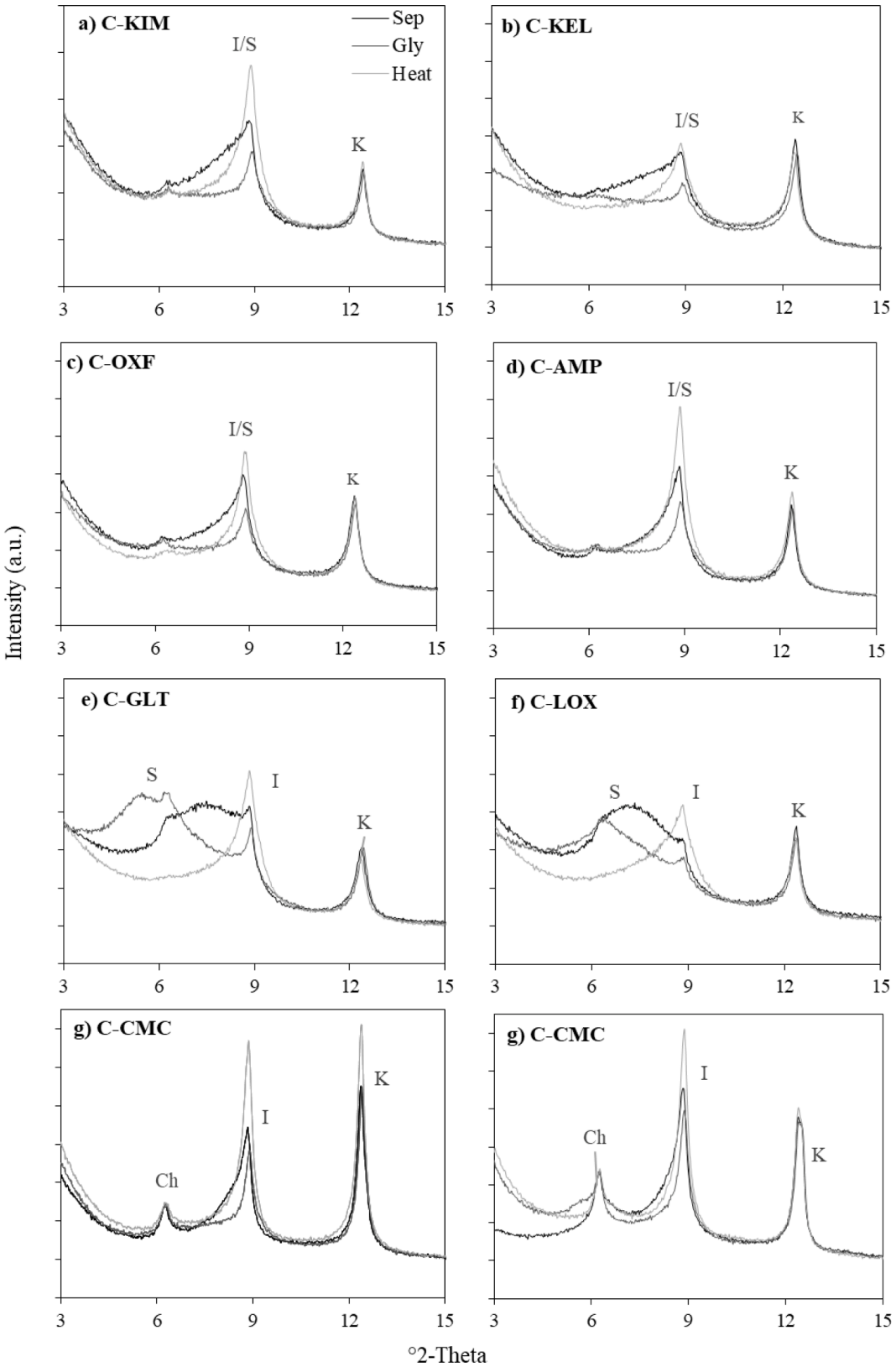

Fig. 3. Identification of clay types: XRD analysis of the samples after separating clay fraction (Sep), treatment with ethylene glycol (Gly) and heating at 400 °C (Heat). Peaks (001 reflections) of the identified phases are marked as I: illite, S: smectite, I/S:illite/smectite, K: kaolinite, Ch: chlorite.

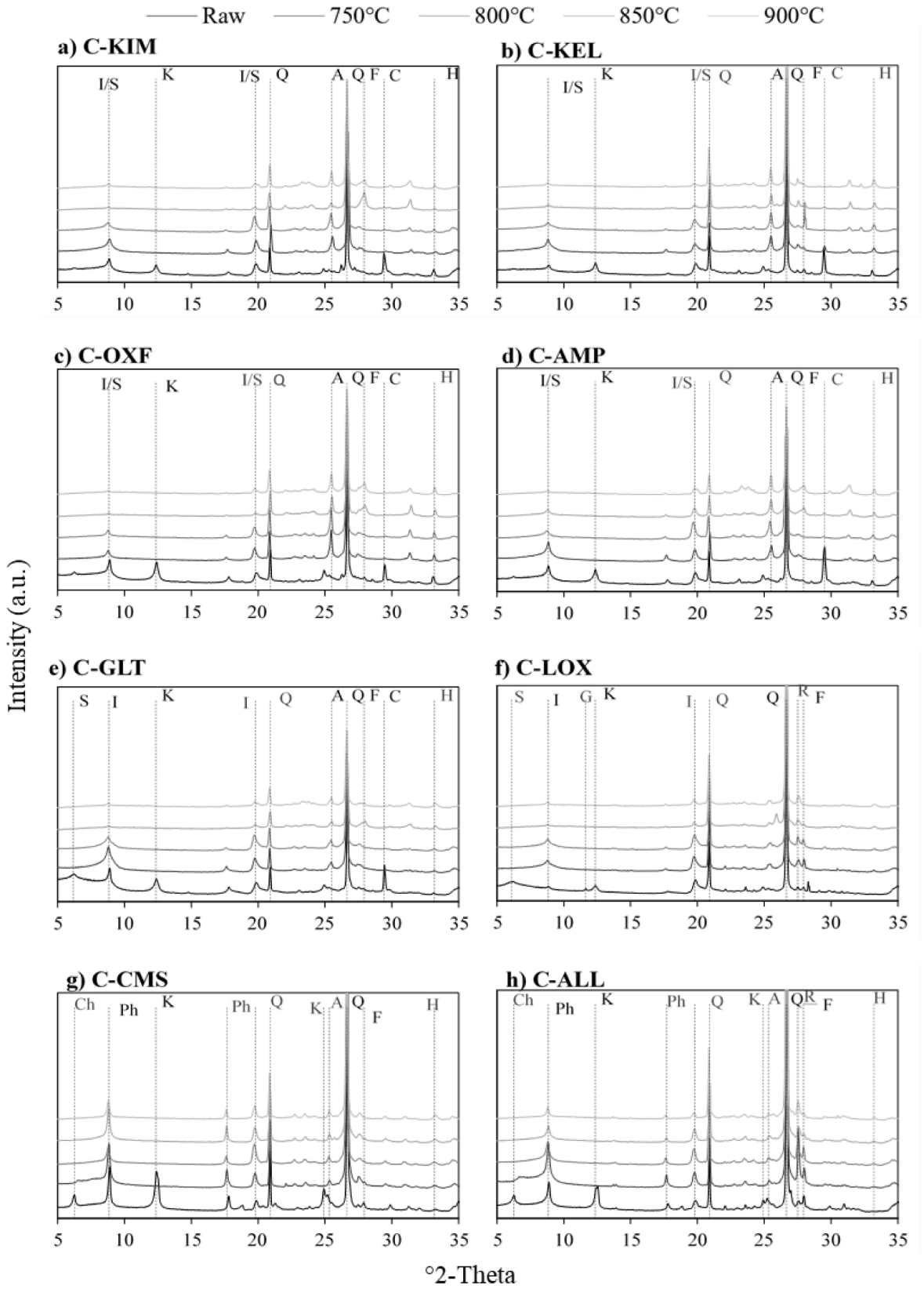

Fig. 4. XRD analysis of clays calcined at 750 °C, 800 °C, 850 °C and 900 °C. Dashed lines marks the position of the high-intensity peak of major phases identified (I: illite, S: smectite, K: kaolinite, Ch: chlorite, Ph: Phlogopite, A: anhydrite, Q: quartz, F: feldspar, C: calcite, H: Hematite, G: gypsum and R: rutile).

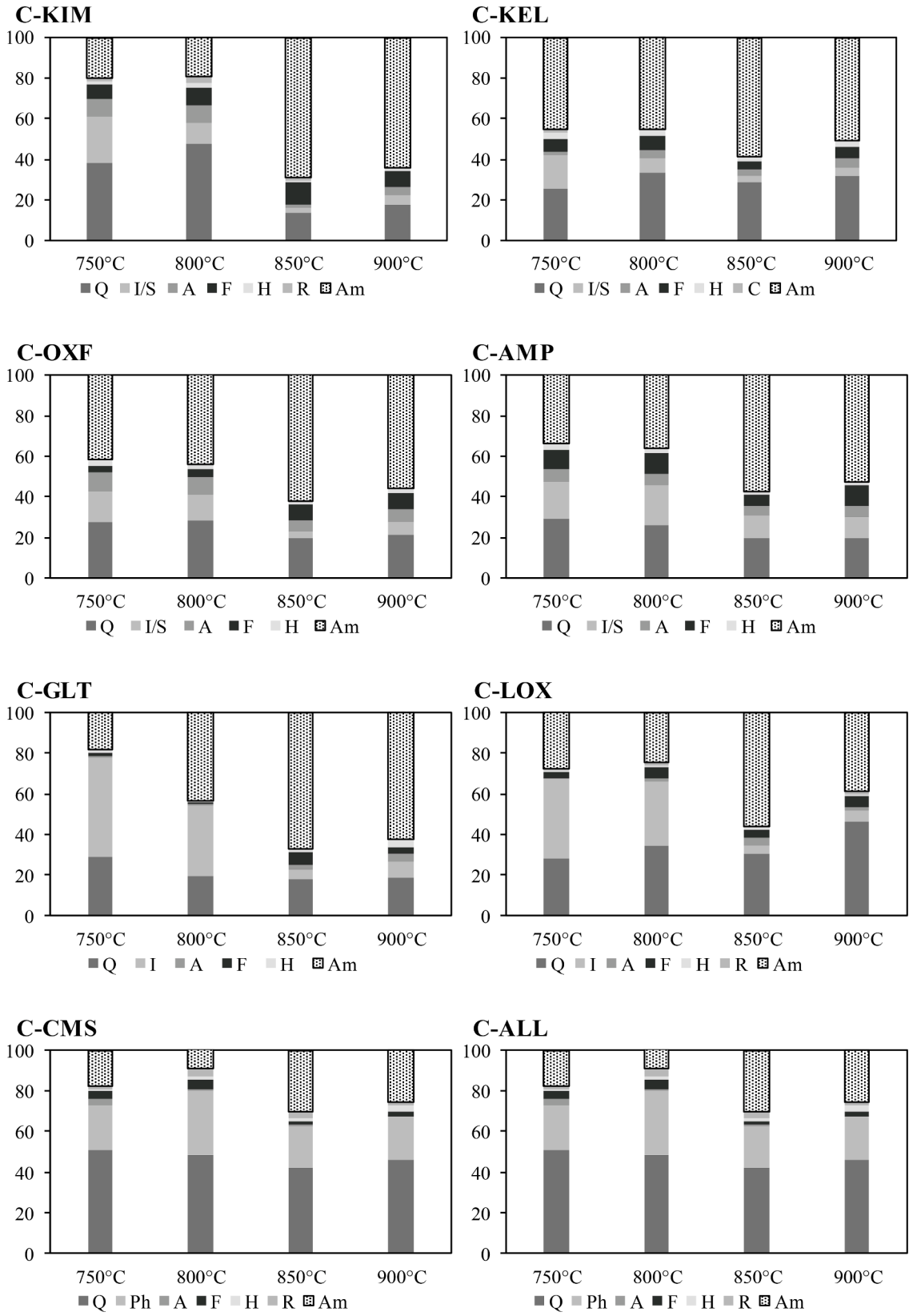

Fig. 5. Mineral phase composition and the amorphous content (A_m) of calcined clays at different temperatures measured using XRD/Rietveld analysis. Phases quantified included quartz (Q), illite (I), smectite (S), chlorite (C), phlogopite (Ph), anhydrite (A), feldspar (F), rutile (R) and hematite (H).

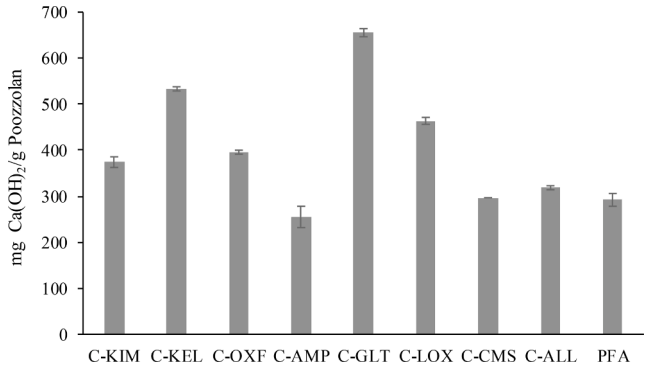

Fig. 6. Measure of the pozzolanic activity of calcined clays (850 °C) determined from the amount of $Ca(OH)_2$ reacted per g of calcined clay using a modified Chapelle test (BS 8615-1).

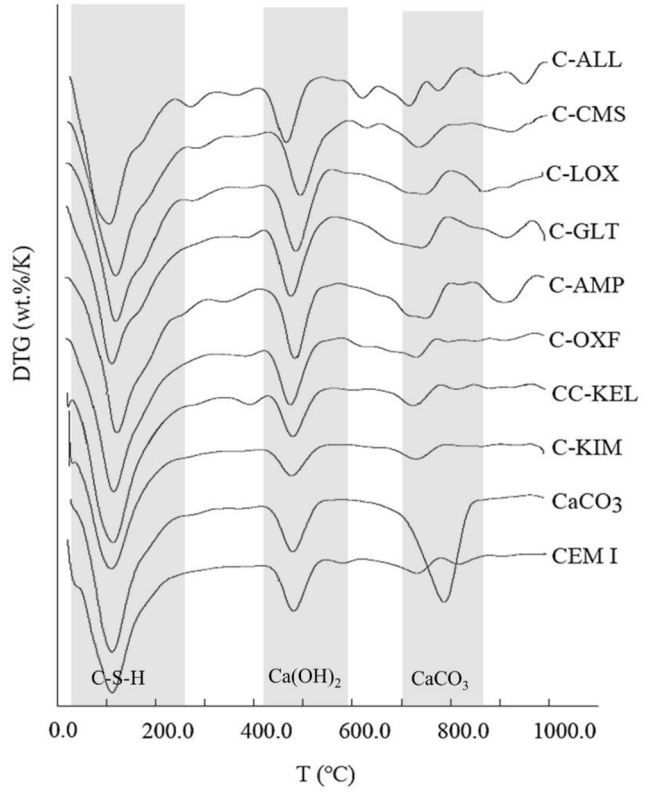

Fig. 7. Derivative thermogravimetry (DTG) curves of 75% PC: 25% calcined clay (850 °C) paste mixes after 28 days of curing showing weight loss peaks in C-S-H, $Ca(OH)_2$ and $CaCO_3$ decomposition temperature ranges. Plain PC (CEM I) and 75% PC: 25% $CaCO_3$ mixes were used as controls.

identified as the major non-clay phases.

XRD data and phase composition of clays after calcining at 750, 800, 850 and 900 °C are shown in Fig. 4 and Fig. 5. A complete dehydroxylation of kaolinite was detected after calcining at 750 °C. The smectite phase in C-GLT and C-LOX, and the chlorite in C-CMS and C-ALL also underwent decomposition at 750 °C. The mixed-layer I/S content in C-KIM, C-KEL, C-OXF and C-AMP exhibited a sharp decrease when the calcining temperature increased above 800 °C while illite and phlogopite remained in calcined clays even until 900 °C. The decomposition of clay minerals mainly resulted in the formation of an amorphous phase.

Fig. 5 shows an increase in the amorphous phase content (W_{AM}) of calcined clays with calcining treatment up to 850 °C, followed by a reduction at 900 °C, due to formation of new crystalline phases. This is in agreement with other studies on illite and smectite rich clay, where 850 °C was reported as the optimal calcining temperature (Danner et al., 2018). Calcination at 850 °C is highly effective for increasing W_{AM} in C-KIM (69.1%), C-KEL (58.4%), C-OXF (62.1%), C-AMP (57.1%) and C-GLT (67.0%) to comparable levels to those found in PFA (75.4%). The major crystalline phase formed in calcined clays was feldspar (anorthite – $CaAl_2Si_2O_8$) while anhydrite ($CaSO_4$) and hematite (Fe_2O_3) were detected in calcined clays originally containing calcite ($CaCO_3$) and pyrite (FeS_2).

Pozzolanic activity of calcined clays

Fig. 6 shows the $Ca(OH)_2$ fixed by clays calcined at 850 °C (mg/g). BS 8615-2 requires the fixation of ≥ 600 mg/g for a high reactivity natural calcined pozzolana suitable for use in combination with PC. C-GLT produced a pozzolanic activity of 655.3 mg/g. Although the calcined clays from other sources did not meet the ≥ 600 mg/g requirement, they did produce pozzolanic activities either in same range or above the levels measured for PFA of 292.1 mg/g. Nevertheless, the pozzolanic activity obtained through the BS 8615-1 method should be treated with caution as the results often do not correlate well with compressive strength because sulphate and alkali levels are different to those of the chemical environment within hydrating cementitious blends (Avet et al., 2016).

Thermogravimetry

Fig. 7 shows DTG data of 75% PC: 25% calcined clay paste mixes after 28 days of curing. The data showed distinctive weight loss in the regions of calcium-silicate-hydrate C-S-H (50–250 °C), $Ca(OH)_2$ (450–600 °C) and $CaCO_3$ (700–850 °C) decomposition. Fig. 8 shows the remaining $Ca(OH)_2$ (wt.%) in the samples after 28 days calculated from DTG curves, as a measure for the pozzolanic activity. The $Ca(OH)_2$ content of plain PC was 25.1% and 24.3% after 7 and 28 days of hydration. This reduced to 21.2% and 22.0% after 7 and 28 days in the 75% PC: 25% $CaCO_3$ sample due to dilution effects. The increase in $Ca(OH)_2$ in this sample with time is because of the filler effect where the $CaCO_3$ particles provide nucleation sites for hydration. However, this was not the case for calcined clays. The $Ca(OH)_2$ content of pastes containing C-KIM, C-KEL, C-OXF, C-AMP, C-GLT, and C-LOX reduced to 17.7%, 18.0%, 17.0%, 19.3%, 19.0% after 28 days of hydration indicating the progress of pozzolanic activity. Clay samples C-OXF and C-AMP from the Oxford and Ampthill geological formation exhibited the highest pozzolanic activity. This was due to generation of significant amounts of amorphous phase capable of reacting with $Ca(OH)_2$. C-CMS and C-ALL had the lowest pozzolanic activity, in the range of PC:$CaCO_3$ sample. This was due to the presence thermally stable phlogopite ($KMg_3(AlSi_3O_{10})(F,OH)_2$), as the dominant clay producing the lowest amorphous phase in these samples (Figs. 4 and 5).

Strength activity index

Fig. 9 shows the SAI of mortar cubes containing 25% calcined clay (850 °C) measured after 28 days. The compressive strength of samples with 100% PC was in the range between 50 and 55 MPa. The measured SAIs for cubes with C-OXF (90.3%) and C-AMP (89.6%) were the highest and were higher than those for PFA. Cubes containing 25% $CaCO_3$ had a SAI of 76.6%, which was mainly due to the dilution effect. An improved correlation between SAI and pozzolanic activity measured from DTG data was observed.

Discussion

This paper investigated low-grade clay samples from clay deposits with different geological formations across the UK. Illite, smectite and mixed-layered I/S were the most prevalent clay minerals while kaolinite

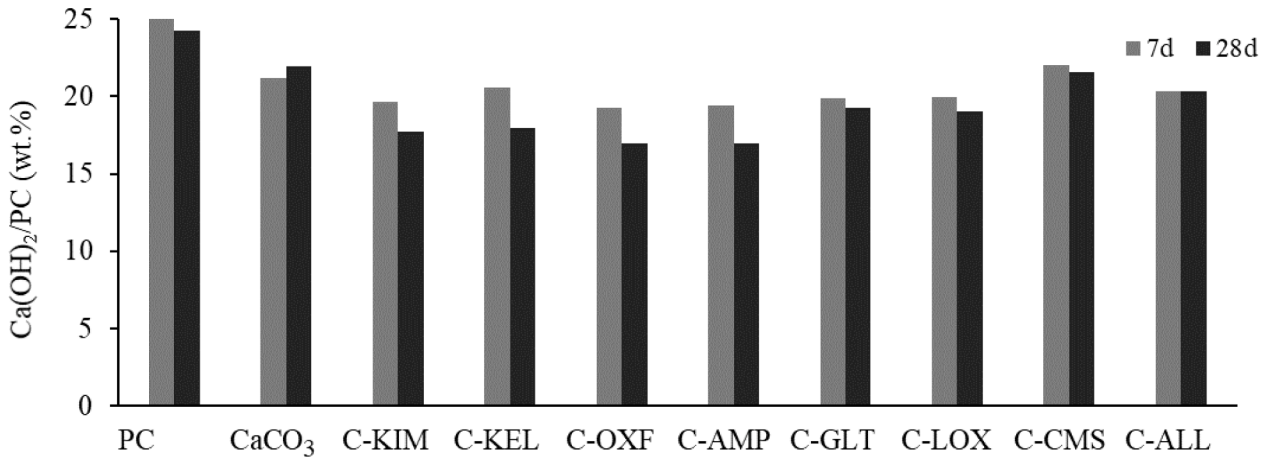

Fig. 8. $Ca(OH)_2$ content of 75% PC: 25% calcined clay (850 °C) paste mixes after 7 and 28 days of curing calculated from DTG curves. $Ca(OH)_2$ content of plain PC and 75% PC: 25% $CaCO_3$ mixes are shown to account for the filler and dilution effects.

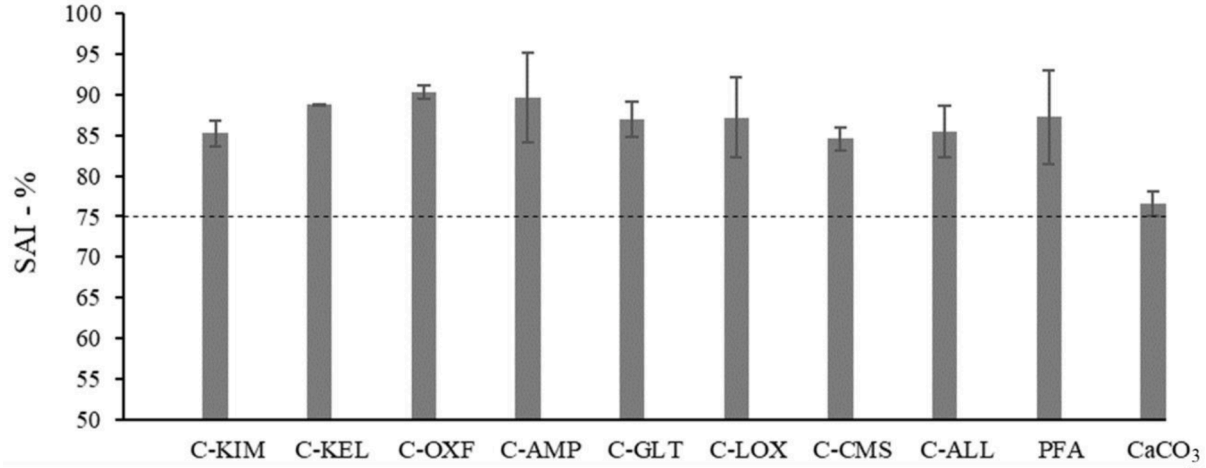

Fig. 9. Strength activity index (SAI) of 75% PC: 25% calcined clay (850 °C) mortars at 28 days at w/b ratio of 0.5. SAI of a 75% PC: 25% $CaCO_3$ mix is shown to account for the filler and dilution effects. The SAI 75% line indicates the EN 450-1 requirement for pozzolanic activity after 28 days.

and chlorite were present at lower concentrations. The study showed that such mineral compositions can produce a significant pozzolanic activity because most of the clay minerals present in the raw materials were capable of transforming into a reactive amorphous phase when subjected to sufficient thermal energy activation.

The highest amorphous content was generated at 850 °C in all clay samples. The variation in the amorphous content was related to the total clay minerals present in the raw materials. The amorphous content is often used to predict the reactivity of SCMs. However, the intrinsic reactivity of the amorphous phase depends on factors such as the chemical compositions and the degree of glass polymerisation (Skibsted and Snellings, 2019). This could explain the observed discrepancies in the prediction of pozzolanic activity tests (Chapelle test, TGA and SAI) based only on the total amorphous content. The heterogeneous mineralogy of clays affect these factors and therefore reactivity of the calcined clays.

Despite the heterogeneous nature of the clays and the variety of geological formations studied, common trends in phase transformation upon calcining was observed and the output solids had relatively similar mineral compositions. Most notably were the formation of feldspars and anhydrite the quantity of which were closely related to the calcite and pyrite content in the raw materials, respectively. The reaction of CaO from decomposition of calcite and the clay alumino-silicate phase at high temperatures has been reported to form non-reactive phases such as gehlenite, wollastonite and anorthite and affect the performance of calcined clays in cement (Traore et al., 2003). The XRD analysis confirmed the formation feldspars at low quantities, but gehlenite or wollastonite were hardly detectable. It must be noted that while no evidence for the formation of crystalline lime or amorphous calcium carbonate was observed, the incorporation of calcium in the amorphous alumino-silicate phase could not be ruled out. In addition, the remaining calcite in clays calcined at 800 °C or lower can reduce the reactivity by reducing the SSA (Danner et al., 2020; Zunino et al., 2020). Calcining the clays at 850 °C ensured the full decomposition of calcite to prevent such effect.

The presence of other non-clay impurities such as quartz and pyrite affected the reactivity of calcined clay in different ways. Quartz is present in clays as hard particles that are more difficult to grind than clays. This is seen in the lower fineness of calcined clays (45 μm residue of 30–50%) compared to PFA (45 μm residue of 8.4%), although the SSAs are in a similar range (1–1.5 m^2/g) as shown in Table 2. The presence of quartz in the range of 20–40% can accelerate the rate of hydration reactions depending on the particle size and surfaces provided due to a filler effect (Kumar et al., 2017). However, samples with high quartz content exhibit dilution as the increase in nucleation sites is low compared to the surface area provided (Berodier et al., 2014). Anhydrite was detected in clays originally containing pyrite. Although anhydrite content in clays calcined at above 800 °C was <5%, its presence can

affect the cement hydration and stability of AFm and Aft phases.

A promising approach to mitigate the adverse role of impurities and to increase the reactivity of calcined clays would be purification of clay materials to increase the clay fraction in raw materials. Clay minerals are usually present in the fine fraction <2 μm and exhibit an advantage in terms of grindability. This can facilitate separation from impurities using accelerated sedimentation by centrifugation or air classifiers found in any grinding unit of current cement plants (Zunino and Scrivener, 2020).

This study demonstrates the potential of low-grade clays to be calcined and used as SCMs. These calcined clays are associated with carbon savings because the optimum calcination temperature of 850 °C is low compared to that used in the manufacture of PC (1450 °C). Low-grade clay deposits can supply raw materials for calcination in large quantities. A great deal of research has been completed on calcined clays due to their availability, low-cost and the simplicity of the manufacturing process. However, there are still uncertainties concerning the viability of the technology as the performance of calcined clays are influenced by mineralogy of the raw materials and carbonation seems to limit the application of calcined clays in concrete (Trümer and Ludwig, 2018). This remains a major barrier to cement manufacturers adopting calcined clays to address the potential shortages of conventional SCMs such as PFA and GGBFS. The issue of long-term durability of cementitious materials containing calcined low-grade clays also needs to be addressed in order to realise the full potential of calcined clays as sustainable low-carbon SCMs for the construction industry.

Conclusions

The ability of low-grade clays (<20% kaolinite) to be calcined to produce supplementary cementitious materials (SCMs) comparable to PFA and GGBFS has been investigated. The study focused on eight UK clay deposits with different geological formations to provide mineralogical variability in raw materials. Clays obtained from Oxford and Ampthill geological formations calcined at 850 °C had high pozzolanic activities from reaction with $Ca(OH)_2$ and strength activity index (~90%) data. These are rich in illite/smectite mixed layered clays, and they produced ~60% reactive amorphous phases after calcining. Non-clay impurities such as calcite, quartz and pyrite are present in clays, and approaches to mitigate their effect on calcined clays reactivity is worthy of further investigation. The research demonstrates that low-grade clay deposits are a readily available resource that can have a key role in satisfying the future demand for low-carbon SCMs.

Declaration of Competing Interest

The authors declare that they have no known competing financial interests or personal relationships that could have appeared to influence the work reported in this paper.

Acknowledgement

The authors would like to thank the support from Tarmac National Laboratory.

Funding

This study has received funding from Tarmac Cement Ltd.

References

Almenares, R.S., Vizcaíno, L.M., Damas, S., Mathieu, A., Alujas, A., Martirena, F., 2017. Industrial calcination of kaolinitic clays to make reactive pozzolans. Case studies in construction materials 6, 225–232.

Avet, F., Snellings, R., Alujas Diaz, A., Ben Haha, M., Scrivener, K., 2016. Development of a new rapid, relevant and reliable (R3) test method to evaluate the pozzolanic reactivity of calcined kaolinitic clays. Cement and Concrete Research 85, 1–11. https://doi.org/10.1016/j.cemconres.2016.02.015.

Ayati, B., Ferrándiz-Mas, V., Newport, D., Cheeseman, C., 2018. Use of clay in the manufacture of lightweight aggregate. Construction and Building Materials 162, 124–131. https://doi.org/10.1016/j.conbuildmat.2017.12.018.

Berodier, E., Scrivener, K., Scherer, G., 2014. Understanding the Filler Effect on the Nucleation and Growth of C-S-H. Journal of the American Ceramic Society 97 (12), 3764–3773.

Brime, C., 2011. S. Fiore, J. Cuadros and FJ Huertas (Editors) (2010) Interstratified Clay Minerals: Origin, Characterization and Geochemical Significance. AIPEA Educational Series, Publication Number 1. Clay Minerals 46, 663–665.

BS EN 196-1: 2005: Methods of testing cement. Determination of strength.

Danner, T., Norden, G., Justnes, H., 2020. The Effect of Calcite in the Raw Clay on the Pozzolanic Activity of Calcined Illite and Smectite BT – Calcined Clays for Sustainable Concrete, in: Bishnoi, S. (Ed.). Springer Singapore, Singapore, pp. 131–138.

Danner, T., Norden, G., Justnes, H., 2018. Characterisation of calcined raw clays suitable as supplementary cementitious materials. Applied Clay Science 162, 391–402. https://doi.org/10.1016/j.clay.2018.06.030.

Environment, U.N., Scrivener, K.L., John, V.M., Gartner, E.M., 2018. Eco-efficient cements: Potential economically viable solutions for a low-CO2 cement-based materials industry. Cement and Concrete Research 114, 2–26.

IEA, W., 2009. Cement Technology Roadmap 2009–Carbon emissions reductions up to 2050. Paris, France 1–2.

International Energy Agency, 2018. Low-Carbon Transition in the Cement Industry [WWW Document]. Technology roadmap for cement.

Kaddatz, K.T., Rasul, M.G., Rahman, A., 2013. Alternative Fuels for use in Cement Kilns: Process Impact Modelling. Procedia Engineering 56, 413–420. https://doi.org/10.1016/j.proeng.2013.03.141.

Kaminskas, R., Monstvilaite, D., Valanciene, V., 2018. Influence of low-pozzolanic activity calcined mica clay on hydration and hardening of Portland cement. Advances in Cement Research 30 (6), 231–239. https://doi.org/10.1680/jadcr.17.00092.

Krishnan, S., Emmanuel, A.C., Shah, V., Parashar, A., Mishra, G., Maity, S., Bishnoi, S., 2019. Industrial production of limestone calcined clay cement: experience and insights. Green Materials 7, 15–27. https://doi.org/10.1680/jgrma.18.00003.

Krishnan, S., Gopala Rao, D., Bishnoi, S., 2020. Why Low-Grade Calcined Clays Are the Ideal for the Production of Limestone Calcined Clay Cement (LC3) BT – Calcined Clays for Sustainable Concrete, in: Bishnoi, S. (Ed.). Springer Singapore, Singapore, pp. 125–130.

Kumar, A., Oey, T., Falzone, G., Huang, J., Bauchy, M., Balonis, M., Neithalath, N., Bullard, J., Sant, G., 2017. The filler effect: The influence of filler content and type on the hydration rate of tricalcium silicate. Journal of the American Ceramic Society 100, 3316–3328. https://doi.org/10.1111/jace.14859.

Li, J., Tharakan, P., Macdonald, D., Liang, X., 2013. Technological, economic and financial prospects of carbon dioxide capture in the cement industry. Energy Policy 61, 1377–1387. https://doi.org/10.1016/j.enpol.2013.05.082.

Madsen, I.C., Scarlett, N.V.Y., Kern, A., 2011. Description and survey of methodologies for the determination of amorphous content via X-ray powder diffraction. Zeitschrift für Kristallographie Crystalline Materials 226, 944–955.

Mirhosseini, M., Rezania, A., Rosendahl, L., 2019. Power optimization and economic evaluation of thermoelectric waste heat recovery system around a rotary cement kiln. Journal of Cleaner Production 232, 1321–1334. https://doi.org/10.1016/j.jclepro.2019.06.011.

Moore, D.M., Reynolds Jr, R.C., 1989. X-ray Diffraction and the Identification and Analysis of Clay Minerals. Oxford University Press (OUP).

Poppe, L.J., Paskevich, V.F., Hathaway, J.C., Blackwood, D.S., 2001. A laboratory manual for X-ray powder diffraction. US Geological Survey open-file report 1, 1–88.

Roussanaly, S., Fu, C., Voldsund, M., Anantharaman, R., Spinelli, M., Romano, M., 2017. Techno-economic Analysis of MEA CO2 Capture from a Cement Kiln – Impact of Steam Supply Scenario. Energy Procedia 114, 6229–6239. https://doi.org/10.1016/j.egypro.2017.03.1761.

Sabir, B.B., Wild, S., Bai, J., 2001. Metakaolin and calcined clays as pozzolans for concrete: a review. Cement and Concrete Composites 23, 441–454. https://doi.org/10.1016/S0958-9465(00)00092-5.

Schulze, S.E., Rickert, J., 2019. Suitability of natural calcined clays as supplementary cementitious material. Cement and Concrete Composites 95, 92–97. https://doi.org/10.1016/j.cemconcomp.2018.07.006.

Scrivener, K., Avet, F., Maraghechi, H., Zunino, F., Ston, J., Hanpongpun, W., Favier, A., 2019. Impacting factors and properties of limestone calcined clay cements (LC3). Green Materials 7, 3–14. https://doi.org/10.1680/jgrma.18.00029.

Scrivener, K., Martirena, F., Bishnoi, S., Maity, S., 2018. Calcined clay limestone cements (LC3). Cement and Concrete Research 114, 49–56. https://doi.org/10.1016/j.cemconres.2017.08.017.

Skibsted, J., Snellings, R., 2019. Reactivity of supplementary cementitious materials (SCMs) in cement blends. Cement and Concrete Research 124, 105799. https://doi.org/10.1016/j.cemconres.2019.105799.

Spinelli, M., Martínez, I., Romano, M.C., 2018. One-dimensional model of entrained-flow carbonator for CO2 capture in cement kilns by Calcium looping process. Chemical Engineering Science 191, 100–114. https://doi.org/10.1016/j.ces.2018.06.051.

Stetsko, Y.P., Shanahan, N., Deford, H., Zayed, A., 2017. Quantification of supplementary cementitious content in blended Portland cement using an iterative Rietveld–PONKCS technique. Journal of Applied Crystallography 50, 498–507. https://doi.org/10.1107/s1600576717002965.

Tironi, A., Cravero, F., Scian, A.N., Irassar, E.F., 2017. Pozzolanic activity of calcined halloysite-rich kaolinitic clays. Applied Clay Science 147, 11–18.

Tironi, A., Trezza, M.A., Scian, A.N., Irassar, E.F., 2013. Assessment of pozzolanic activity of different calcined clays. Cement and Concrete Composites 37, 319–327.

Traore, K., Kabre, T.S., Blanchart, P., 2003. Gehlenite and anorthite crystallisation from kaolinite and calcite mix. Ceramics International 29 (4), 377–383. https://doi.org/10.1175/1520-0450(2003)042<1355:VOTAOR>2.0.CO;2.

Trümer, A., Ludwig, H.-M., 2018. In: Assessment of Calcined Clays According to the Main Criterions of Concrete Durability BT – Calcined Clays for Sustainable Concrete. Springer, Netherlands, Dordrecht, pp. 475–481.

Vizcaíno Andrés, L.M., Antoni, M.G., Alujas Diaz, A., Martirena Hernández, J.F., Scrivener, K.L., 2015. Effect of fineness in clinker-calcined clays-limestone cements. Advances in Cement Research 27, 546–556. https://doi.org/10.1680/jadcr.14.00095.

Wu, W.-N., Liu, X.-Y., Hu, Z., Zhang, R., Lu, X.-Y., 2019. Improving the sustainability of cement clinker calcination process by assessing the heat loss through kiln shell and its influencing factors: A case study in China. Journal of Cleaner Production 224, 132–141. https://doi.org/10.1016/j.jclepro.2019.03.209.

Zhou, D., Wang, R., Tyrer, M., Wong, H., Cheeseman, C., 2017. Sustainable infrastructure development through use of calcined excavated waste clay as a supplementary cementitious material. Journal of Cleaner Production 168, 1180–1192.

Zunino, F., Boehm-Courjault, E., Scrivener, K., 2020. The impact of calcite impurities in clays containing kaolinite on their reactivity in cement after calcination. Materials and Structures 53, 44. https://doi.org/10.1617/s11527-020-01478-9.

Zunino, F., Scrivener, K., 2020. Increasing the kaolinite content of raw clays using particle classification techniques for use as supplementary cementitious materials. Construction and Building Materials 244, 118335. https://doi.org/10.1016/j.conbuildmat.2020.118335.